Experimental and Numerical Analysis of Moisture Transport in Walnut and Cherry Wood in Radial and Tangential Material Directions

Daniel Konopka,[a] Erik V. Bachtiar,[b] Peter Niemz,[b,c] and Michael Kaliske [a,*]

The diffusion properties of walnut (*Juglans regia* L.) and cherry (*Prunus avium* L.) wood perpendicular to the grain are presented. The wet and dry cup tests were carried out in normal climate conditions. Simultaneously, inverse analyses by means of the finite element (FE) method were conducted based on the experimental sorption data. The results show that the numerically derived diffusion model can predict the mass changes during the experiments with sufficient accuracy with a maximum global relative error of 0.43%. However, the numerically determined diffusion coefficients do not show an agreement with the experimental data.

Keywords: Cherry; Walnut; Diffusion coefficient; Moisture dependency; Cup test; Inverse analysis

Contact information: a: Institute for Structural Analysis, Technische Universität Dresden, D-01062 Dresden, Germany; b: Institute for Building Materials, ETH Zurich, 8093 Zürich, Switzerland; c: Institute for Material and Wood Technology, Bern University of Applied Science, 6096 Biel, Switzerland;
** Corresponding author: michael.kaliske@tu-dresden.de*

INTRODUCTION

Valuable hardwood is often used for decorative artworks and frequently found in wooden cultural heritage objects. Walnut and cherry wood were investigated in this work since these species, compared *e.g.* to beech, oak or coniferous wood like spruce, have only been scarcely studied with respect to their moisture transport behavior. The knowledge on these wood species provided by this study can be used for any conservation purpose in the future.

As a hygroscopic material, wood adjusts its moisture to the surrounding conditions by the adsorption or desorption and diffusion of water vapor until it reaches an equilibrium moisture content (EMC) with a steady-state distribution. During this period, which requires days to months depending on the wood specimen size, swelling or shrinking will also occur as wood attaches and detaches the water molecules. In applications where wood is exposed to uncontrolled climatic conditions, extreme and repetitive swelling or shrinkage may damage the wood (Lamb 1992).

The moisture transport/diffusion properties of wood have been studied thoroughly (Klopfer 1974; Siau 1995; Sonderegger *et al.* 2011; Mannes *et al.* 2012). The diffusion properties of wood are experimentally measured in two ways, *i.e.*, transient and steady-state. The transient/unsteady-state method is based on the water adsorption or desorption rate of wood. The diffusion coefficient (D) is estimated based on the change of mass before the wood specimen reaches an EMC. In contrast, the steady-state method calculates D based on the mass of the moisture being transported through the wood with EMC. Because transient conditions often appear at the beginning within the experimental procedure and the steady-state appears later, they are also referred to as short- and long-term moisture

transport conditions, respectively (Sonderegger *et al.* 2011). The diffusion characteristics change during both states. Differences of approximately one order of magnitude may occur, depending on the wood species, the fiber direction, and the moisture difference (Pfriem 2006). In this study, both, unsteady- and steady-state analyses are performed based on the conventional cup method (DIN EN ISO 12572 2001).

Within an inverse analysis of the transient diffusion process, cup test specific moisture-dependent diffusion coefficients $D(m)$ for the numerical analysis in the scope of the finite element method (FEM) were determined in this study. The inverse analysis, which was introduced by Hrcka and Babiak (1999) and Olek *et al.* (2005) for the bound water diffusion coefficient identification in wood, was further adapted for special diffusion experiments on certain wood species (Koc and Houska 2002; Koc *et al.* 2003; Olek *et al.* 2005; Mannes *et al.* 2009; Hering 2011; Olek *et al.* 2011; Sonderegger 2011). With the determined $D(m)$, the experimental test setups can be modelled. The FE-analysis allows insight into the specimens' time-dependent inner moisture distribution over the length section, *i.e.*, the direction of moisture transport. Moreover, the species-dependent coefficients enable a direct quantitative comparison to other similar cup test diffusion experiments, *e.g.*, different wood species, wood products, or composite materials (Sonderegger and Niemz 2009). The same analysis method was applied for scots pine (*Pinus sylvestris* L.), beech wood (*Fagus sylvatica* L.), and Norway spruce (*Picea abies* L.) (Olek *et al.* 2005; Mannes *et al.* 2009; Olek *et al.* 2011), although the quantitative comparison was restricted due to different geometries, humidity levels, and sorption directions (ad-/desorption).

EXPERIMENTAL

Materials and Specimens

The measurements were carried out for two hardwood species, walnut (*Juglans regia* L.) and cherry (*Prunus avium* L.) wood grown in the Caucasus region. The average wood densities for walnut (ρ = 678 ± 60 kg m^{-3}) and cherry (ρ = 550 ± 23 kg m^{-3}) were measured at normal climatic conditions (temperature T = 20 °C, relative humidity RH = 65%). In these conditions, the wood moisture contents were m_{walnut} = 9 ± 0.2% and m_{cherry} = 10 ± 0.2%. The specimens used for the experimental tests were cylindrical wooden discs with a diameter of 140 mm and a thickness of 10 mm (Fig. 1) without any natural growth characteristics such as knots or reaction wood. Of the six specimens that were prepared for each sample type, three samples were tested in dry conditions and the other three in wet conditions (Table 1).

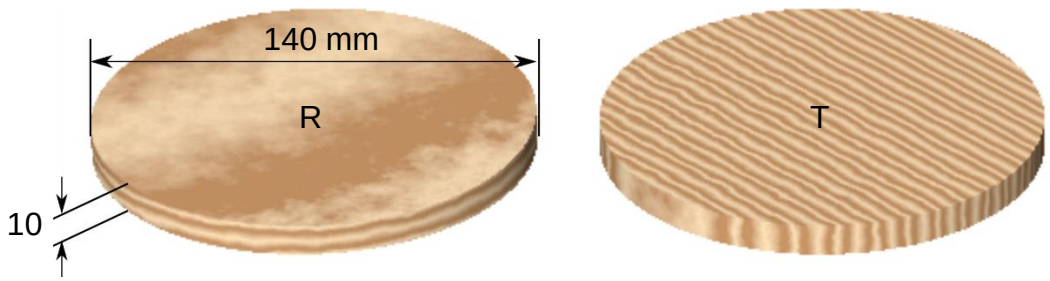

Fig. 1. Water vapor diffusion specimens in radial (R) and tangential (T) direction

Table 1. Tested Specimens

Wood	Direction	Label	ρ(*20 °C/65% RH*)
Walnut	Radial	WR	632 ± 40 kg m^{-3}
	Tangential	WT	725 ± 33 kg m^{-3}
Cherry	Radial	CR	551 ± 28 kg m^{-3}
	Tangential	CT	547 ± 20 kg m^{-3}

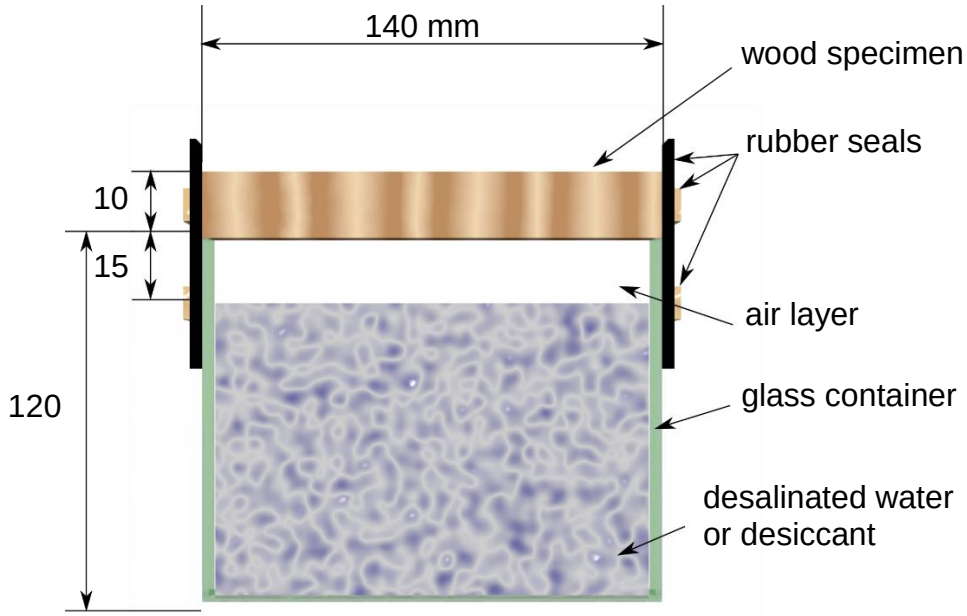

Fig. 2. Test setup: dry cup container filled with desiccants, wet cup container filled with desalinated water. All dimensions are in mm.

Testing Method

Before the tests, all specimens were conditioned under normal climate conditions (20 °C, 65% *RH*) for at least two months. The water vapor uptake investigation combined with the steady-state wet and dry cup diffusion tests based on DIN EN ISO 12572 (2001) were performed in the same ambient climate by using the wood specimens as the lids of the cylindrical glass containers. The containers with a height of 120 mm and an outer diameter of 140 mm were filled with either desiccant, *i.e.*, silica gel/SiO_2 (dry cup), or desalinated water (wet cup) and an air layer of 15 mm (Fig. 2). Tight rubber seals were used to seal the area between the specimens and their containers. Hence, the water vapor could only transmit (in or out of the containers) through the specimens in one material direction (Sonderegger and Niemz 2009).

All variables used in calculations are defined in Table 2.

As soon as the specimens were placed, their moisture contents slowly adjusted to their new environment (dry on one side and wet on the other side). During this period, the adsorption and desorption rates of the specimens were not equal. The water vapor sorption of the wood specimens (without containers) was observed by a regular mass measurement.

Table 2. List of Symbols

Symbol	Unit	Definition
A_{bw}	kg m^{-2} s$^{-0.5}$	water sorption coefficient of bound water
Δm	kg	mass gain
t	s	time
D_{US}	m^2 s^{-1}	unsteady-state diffusion coefficient
Δc	kg m^{-3}	water concentration difference
g	kg m^{-2} s^{-1}	water vapor transmission rate per surface area
G	kg s^{-1}	water vapor transmission rate, estimated by the gradient of linear regression between the change of total mass (second stage) and time
A	m^2	transmission surface area, estimated by the average of the specimen surface area and the containers opened area
W_c	kg m^{-2} s^{-1} Pa^{-1}	water vapor transmission coefficient
Δp_v	Pa	difference of saturated water vapor pressure across the specimen, estimated by Eq. 8; inside the cups the humidity was assumed to RH = 5% (dry) and RH = 95% (wet), outside the cups RH = 65%
d_a	m	thickness of air layer (Fig. 2)
μ	-	water vapor resistance factor
d	m	specimen thickness
V	m^3	specimen volume at normal climate
w_0	kg	specimen oven-dry mass
ΔH	%	difference of relative humidity across the specimen; inside the cups the humidity was assumed to RH = 5% (dry) and RH = 95% (wet), outside the cups RH = 65%
ΔM	%	difference of moisture content across the specimen measured basing on Table 3
D_{SS}	m^2 s^{-1}	steady-state diffusion coefficient
s_d	m	water vapor diffusion-equivalent air layer thickness
p_v	kg m^{-2} s^{-1}	saturated water vapor pressure
δ_a	kg m^{-1} s^{-1} Pa^{-1}	water vapor permeability of air with respect to the partial vapor pressure
RH	-; %	relative humidity
T	K	temperature (absolute)
p_0	Pa	normalized (sea-level) air pressure, p_0 = 101325 Pa
p	Pa	average air pressure during the measurement period depending on the altitude and climate
R_v	J kg^{-1} K^{-1}	gas constant for water vapor, R_v = 462 J kg^{-1} K^{-1}
q_m	kg mm^{-1} s^{-1}	moisture flux
ρ_0	kg mm^{-3}	dry density of wood for m = 0
ρ	kg mm^{-3}	density of wood (moisture dependent)
D	mm^2 s^{-1}; m^2 s^{-1}	diffusion coefficient
D_0	mm^2 s^{-1}	reference diffusion coefficient
m	-; %	moisture content (local)
m_{end}	-	m for $t = t_{end}$ at the wooden surface inside the cup
MC	-; %	moisture content (global, total specimen)
MC_{end}	-; %	MC for $t = t_{end}$
α	-	factor for m (see Table 5)
S	mm s^{-1}	surface emission coefficient
X	-	vector of optimization parameters
S_r	-	objective function (sum of squared residuals)
e	%	global relative error
x	mm	coordinate in the specimens thickness direction (length section)

Removal, mass measurement, and re-installation were quickly performed one by one for each specimen. The mass was also used as a parameter to determine whether the specimens had reached equilibrium conditions or not. The next experimental state, *i.e.*, the steady-state water vapor diffusion could only be continued once equilibrium was reached. The unsteady-state/transient diffusion coefficients were calculated based on the ad- and desorption data (Klopfer 1974). The water sorption coefficients of bound water (A_{bw}) were calculated as,

$$A_{bw} = \frac{\Delta m}{A \cdot \sqrt{t}} \qquad [\text{kg m}^{-2}\ \text{s}^{-0.5}]. \tag{1}$$

Therefore, the diffusion coefficients (D_{US}), which are assumed to be constant at the beginning of the measurements, are calculated as,

$$D_{US} = \left(\frac{A_{bw}}{\sqrt{4/\pi} \cdot \Delta c} \right)^2 \qquad [\text{m}^2\ \text{s}^{-1}]\ . \tag{2}$$

After 20 days, the specimens reached their EMC. In this state, the permeation of water vapor became a constant process with the three simultaneous main transport phenomena:

1. adsorption of water vapor from higher humidity environment into the wood,
2. diffusion of water through the wood,
3. desorption of water on the opposite surface of the wood to lower humidity environment.

The mass of combined wood specimen and container (whole system) was measured regularly. It is assumed that every mass change of the system was due to the transmission of water in or out of the cup through the wood. The measured data are used to estimate water vapor diffusion properties. This measurement was conducted for approximately 14 days. According to DIN EN ISO 12572 (2001), the diffusion parameters that can be estimated based on the experimental data are water vapor transmission rate per surface area (g),

$$g = \frac{G}{A} \qquad [\text{kg m}^{-2}\ \text{s}^{-1}] \tag{3}$$

water vapor transmission coefficient (W_c) corrected by the air layer between the base of the specimen and the desiccant or water (see Fig. 2),

$$W_c = \left(\frac{\Delta p_v}{g} - \frac{d_a}{\delta_a} \right)^{-1} \qquad [\text{kg m}^{-2}\ \text{s}^{-1}\ \text{Pa}^{-1}] \tag{4}$$

water vapor resistance factor (μ),

$$\mu = \frac{\delta_a}{W_c \cdot d} \qquad [-] \tag{5}$$

diffusion coefficient (D) based on Siau (1995),

$$D_{SS} = \frac{\delta_a \cdot p_v \cdot V}{w_o} \frac{\Delta H}{\Delta M} \qquad [\text{m}^2\ \text{s}^{-1}] \tag{6}$$

and water vapor diffusion-equivalent air layer thickness (s_d),

$$s_d = \mu \cdot d \qquad [\text{m}]. \tag{7}$$

Additionally, complemented parameters required in Eqs. 3 to 7 are saturated water vapor pressure (p_v)

$$p_v = 610.5 \cdot RH \cdot e^{\left(\frac{17.269 \cdot (T-273)}{T-35.7}\right)} \qquad [\text{kg m}^{-2}\ \text{s}^{-1}] \qquad (8)$$

and water vapor permeability of air with respect to the partial vapor pressure,

$$\delta_a = \frac{0.083 \cdot p_o}{R_v \cdot T \cdot p}\left(\frac{T}{273}\right)^{1.81}\frac{1}{3600} \qquad [\text{kg m}^{-1}\ \text{s}^{-1}\ \text{Pa}^{-1}]. \qquad (9)$$

Table 3. Sorption Isotherm Data

MC(*RH*) [%]	5% *RH*	65% *RH*	95% *RH*
Walnut	2.0	8.8	20.0
Cherry	2.3	10.0	20.6

Inverse Analysis of the Diffusion Coefficients

Within the scope of numerical FE-analyses, the diffusion parameters are modelled as a function of moisture. A single discrete material point at a certain time relates to a certain moisture and a diffusion coefficient. In contrast, the experimentally determined steady- and unsteady-state diffusion coefficients only estimate the average values over the entire specimens. Therefore, by integrating the numerically estimated diffusion parameters over the thickness at a certain time, both experimental and numerical are comparable.

Material Model

Fick's second law for the description of the moisture transport in solid materials [see *e.g.* (Crank 1975; Hanhijarvi 1997)] is used assuming a single-phase diffusion. The assumption of Fick's law is valid in the simulation of steady-state transport processes. The transient form, however, often leads to divergence of simulation and experiment, denoted as "non-Fick'ian-behavior" (Wadso 1994). Moisture flux (q_m) is proportional to the gradient of moisture content (m), the diffusion coefficient (D), and the density in absolute dry conditions (ρ_0) serve as constants of proportionality

$$\boldsymbol{q}_m = -\rho_0 \underline{\boldsymbol{D}} \nabla m \,. \qquad (10)$$

The time-dependent form of Fick's law,

$$\frac{\partial m}{\partial t} = \nabla\left(\underline{\boldsymbol{D}}\ \nabla \mathrm{m}\right) \qquad (11)$$

for transient simulations merely gives an approximation of the real transport behavior.

For the internal transport, different approaches in modelling the diffusion coefficient (D) were tested for the configuration WT dry (*cf.* Table 1). The steady-state values determined in the Section "Testing Method" were compared to constant, linear, and the following exponential moisture-dependent approach

$$D(m) = D_0 \cdot \exp(\alpha \cdot m) \qquad [\text{mm}^2\ \text{s}^{-1}], \qquad (12)$$

with moisture content m [-]. As analyzed in Hering (2011), a more complex polynomial exponent is not suggested. The two optimization parameters D_0 and α are considered for the exponential formulation. In the linear approach, two variables are necessary, too,

whereas in the constant approach only D_0 is captured (see Section "Results and Discussion"). Besides the optimized configurations WT1 to WT3, further models were tested. In configurations WT4 and WT5, the constant D of the experimental result was combined with different final equilibrium moisture contents at the inner cup surface m_{end}, originating either from a linear distribution assumption (Sonderegger 2011), or optimization result of configuration WT1. In WT6 and WT7, a micro-structural approach for the determination of steady-state diffusion coefficients of walnut used in (Eitelberger 2011; Reichel 2015) was selected for comparison purposes.

The changing climate was caused by the inner cup conditions. Thus, only the surface emission coefficient (SE-coefficient) on the inner surface is considered as a Neumann boundary condition,

$$q_m = S \cdot (RH^s - RH^{air}) \tag{13}$$

with the SE-coefficient (S), the potential between the relative humidity on the bulk materials surface RH^s [-] and the air inside the cup RH^{air} [-].

As comprehensively studied by Reichel (2015), no reliable knowledge is available on the characteristics of SE. Although, numerous experimental studies and material models are published, it is not possible to derive consistent emission properties. Thus, according to *e.g.* (Olek *et al.* 2005; Mannes *et al.* 2009; Eitelberger 2011; Olek *et al.* 2011) for the limitation of the number of optimization parameters, S is approximated as constant, *i.e.* m-independent. Time-dependency, like in Olek *et al.* (2011) due to reorganization processes of the wood ultra-structure, is neglected.

The sorption behavior is considered by an isotherm model published in Avramidis (1989),

$$m = 0.01 \cdot \left[\frac{-T \cdot ln(1 - RH)}{0.13 \cdot \left(1 - \frac{T}{647.1}\right)^{-6.46}} \right]^{\frac{1}{110} T^{0.75}} \quad [-] \tag{14}$$

with relative humidity RH [-] and temperature T [K]. The applied regression coefficients are derived for a general and wood species independent formulation and used for both wood species in this study.

Numerical Analysis

In pre-simulations with various different FE-models, the highest accuracy with a minimum number of degrees of freedom (DOF) was obtained by modelling the cup specimens with one 20-node solid element over the whole thickness using a quadratic shape function (Bathe 2002) combined with a convective element on the inner surface, which is exposed to the climate change. The pre-study (see Fig. 3) showed that a finer discretization only increased the computational effort without any significant increase in accuracy. Although, for the analysis of the internal moisture distribution a finer discretization is recommended, as discussed in the Section "Results and Discussion", it is not required for the correct average moisture content determination.

The samples' average moisture content (MC) is determined by integrating the shape function of the bound water content (m) along the length section (specimen thickness).

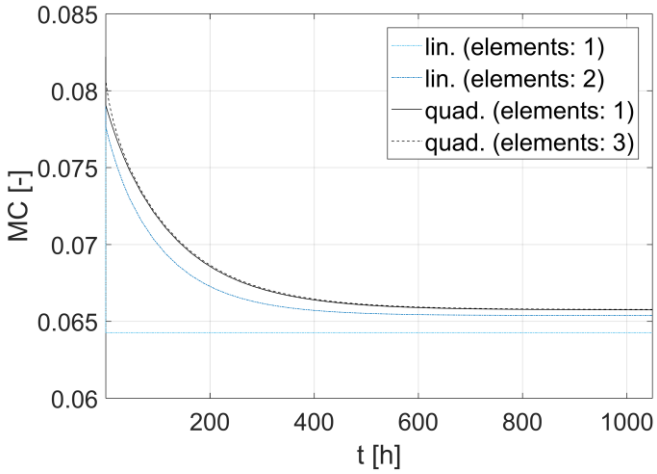

Fig. 3. Comparison of the accuracy in *MC*(*t*)-determination with linear and quadratic shape functions and different discretizations of the FE-model

The inverse analysis optimization is carried out using an internal algorithm coupled to the in-house WoodFEM software. The set of optimization parameters (X) contains a maximum of four variables,

$$X = [D_0, \alpha, m_{end}, S] \tag{15}$$

including the two parameters for Eq. 12, the final water content at the inner cup surface (m_{end}), and a constant SE-coefficient (S). Although the experimental conditions for the cup climate are defined (see Section "Testing Method"), m_{end} is regarded as an optimization variable as well.

The optimization method leads to the minimum of the objective function (S_r), which was chosen as the sum of squared residuals of the experimentally and numerically determined specimens' average moisture contents (MC [-]) at measurement times (t_i)

$$S_r = \sum_{i=1}^{n} \left| MC_{exp}(t_i) - MC_{FEM}(t_i) \right|^2 . \tag{16}$$

Due to the larger number of experimental data at the beginning, there is a higher weight on these results, which is a positive effect for the fitting of the numerical calculation. It means, that during the more pronounced non-equilibrium, which is dependent on the inner moisture distribution, more points for Eq. 16 are provided. This helps to decrease possible inaccuracies by not measuring the inner moisture distribution with the applied experimental method, described in the Section "Testing Method". The optimization is performed *via* a bound constrained optimization based on a trust region approach, since it was found to be the most efficient one for this purpose. Finally, a global relative error [*e.g.* (Olek *et al.* 2011)] in relation to the experimental results can be calculated as:

$$e = 100 \frac{\sqrt{S_r}}{\sqrt{\sum_{i=1}^{n} MC_{exp}(t_i)^2}} \quad [\%]. \tag{17}$$

RESULTS AND DISCUSSION

The results for the global parameters of the specimens, determined as described in Sections "Testing Method" and "Inverse Analysis of the Diffusion Coefficients" are documented in Table 4. Small differences of the experimental diffusion coefficients (D_{us} and D_{ss}) were observed for cherry wood comparing the material directions T and R. The same behavior is known from other wood species, *e.g.* spruce and beech wood (Koc *et al.* 2003; Sonderegger *et al.* 2011). However, the diffusion coefficient (D) of WT showed a significantly lower value in comparison to D of WR. One main issue would be the high density difference between T and R specimens of walnut wood (Table 1). Moreover, D is also dependent on the moisture potential within the specimens (ΔM). Wet cups with a higher potential [difference between MC(*95% RH*) and MC(*65% RH*), see Table 3] tend to have higher D in comparison to dry cup [difference between MC(*5% RH*) and MC(*65% RH*)]. Furthermore, the experimentally determined steady-state diffusion coefficients (D_{SS}) mostly do not show good correlation to the unsteady-state/transient ones (D_{US}). These findings correspond to those of other publications, *e.g.* (Wadso 1994; Pfriem 2006; Sonderegger 2011).

Table 4. Experimentally Determined Steady-State (D_{SS}) and Unsteady-State (D_{US}), and Inversely Determined $D(MC_{end})$ for the Specimens' Global Moisture Content MC_{end}

		MC_{end} [%]		D_{US}		D_{SS}	$D(MC_{end})$	$D(MC_{end})/D_{SS}$-1
		experi-mental	numeri-cal	[m^2 s^{-1}]				[%]
WT	Dry	6.5	6.5	1.1E-11		1.9E-11	2.1E-11	10
	Wet	17.1	18.0	1.4E-10		2.9E-11	1.2E-11	-59
WR	Dry	7.0	6.9	1.1E-11		3.2E-11	4.7E-11	45
	Wet	17.7	17.8	2.4E-10		6.4E-11	2.8E-11	-55
CT	Dry	8.4	8.4	1.2E-11		5.0E-11	5.3E-11	6
	Wet	18.4	18.4	1.9E-10		1.2E-10	4.4E-11	-63
CR	Dry	8.4	8.4	1.1E-11		7.6E-11	1.0E-10	36
	Wet	17.3	17.2	1.6E-10		1.5E-10	5.2E-11	-66

The results of the determination of an accurate approach for $D(m)$, based on the reference sample WT dry (walnut, tangential diffusion, dry cup) are presented in Fig. 4 with the corresponding results of the unknown variables in Table 5. The most accurate approach was the exponential configuration WT1 (S_r=1.059E-6). The assumption of a linear moisture distribution over the samples length (thickness) $m(x,t)$ in the final state (configurations WT4 and WT6) with higher corresponding m_{end} [*cf.* Sonderegger 2011] led to a larger deviation.

While the predictions of $MC(t)$ showed good agreement, the time-dependent moisture distribution within the specimen $m(x,t)$ cannot be validated with the present experimental results. In comparison to other validated investigations, *e.g.* (Mannes *et al.* 2009), $m(x,t)$ showed a qualitatively good comparison.

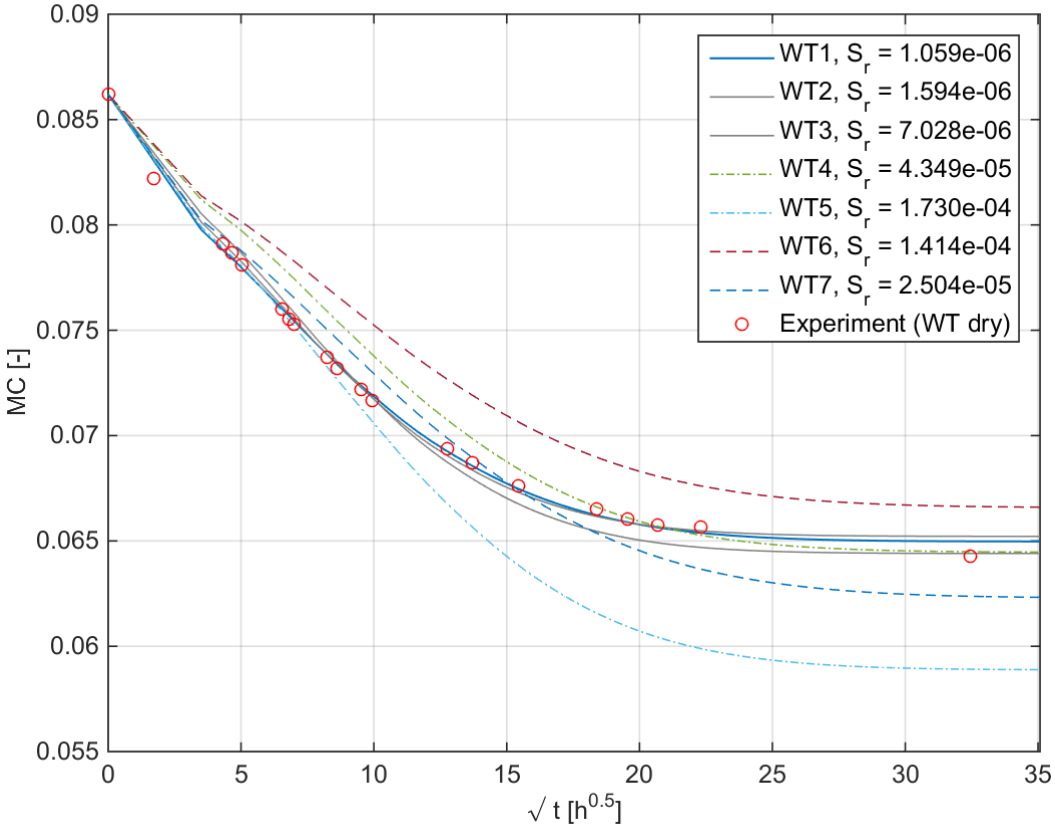

Fig. 4. Accuracy of different diffusion coefficient models $D(m)$ (Table 5)

The distribution with respect to time and the shape of the steady-state condition in equilibrium remains uncertain since the profile of $m(x,t)$ is strongly affected by the diffusion coefficient $D(m)$. Further investigations shall visualize the effects on the internal conditions.

Table 5. Diffusion Coefficients $D(m)$

Test	Diffusion approach	D_0	α	m_{end}	S	notes
		[mm² s⁻¹]	[-]	[-]	[mm s⁻¹]	
WT1	$D(m)=D_0\cdot\exp(\alpha\cdot m)$	3.57E-6	27.51	0.031	2.22E-4	optimization (Eq. 15): $X=[D_0,\alpha,m_{end},S]$
WT2	$D(m)=D_0+\alpha\cdot m$	1.94E-11	4.21E-4	0.038	3.27E-4	optimization (Eq. 15): $X=[D_0,\alpha,m_{end},S]$
WT3	$D(m)=D_0$	2.86E-5	-	0.042	4.42E-4	optimization (Eq. 15): $X=[D_0,\alpha,m_{end},S]$
WT4	$D(m)=D_0$	2.04E-5	-	0.042	2.22E-4	D_0: Table 4
WT5	$D(m)=D_0$	2.04E-5	-	0.031	2.22E-4	D_0: Table 4
WT6	$D(m)=D(m,\rho_0,species)$	1.02E-4	-	0.042	2.22E-4	D_0: micro-model (Eitelberger 2011; Reichel 2015)
WT7	$D(m)=D(m,\rho_0,species)$	1.02E-4	-	0.031	2.22E-4	D_0: micro-model (Eitelberger 2011; Reichel 2015)

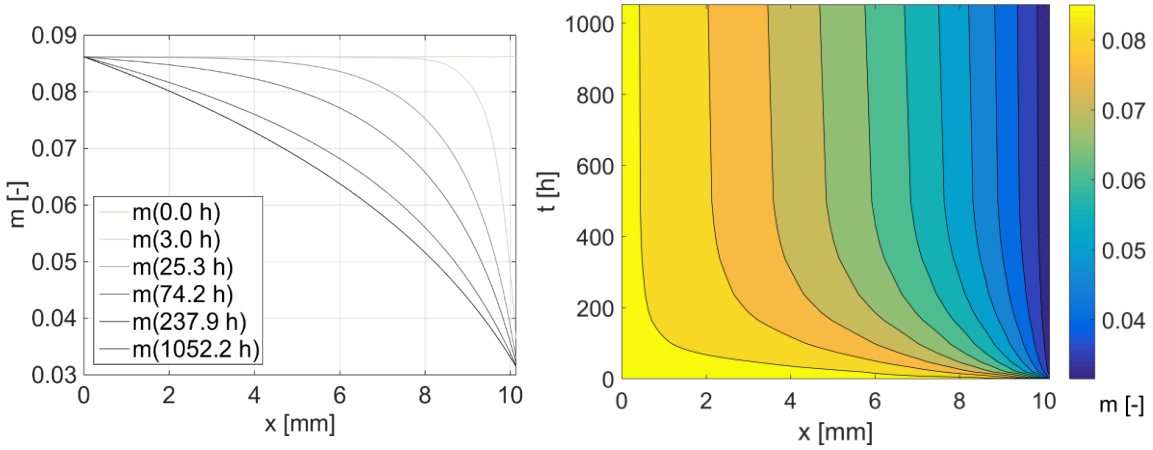

Fig. 5. Distribution of moisture content $m(x,t)$ over length section x for specific experimental times (left) and as density plot (right)

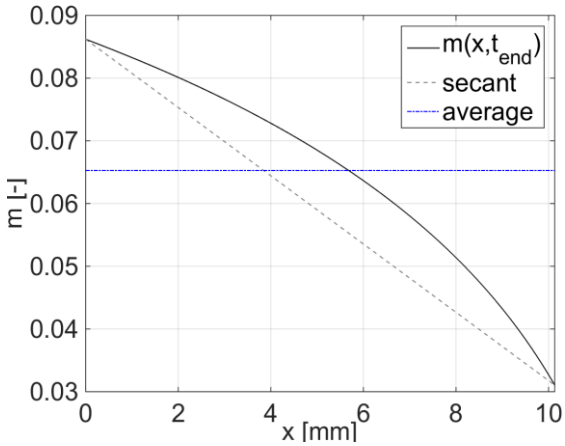

Fig. 6. $m(x,t_{end})$ in steady-state conditions together with its secant and its average value

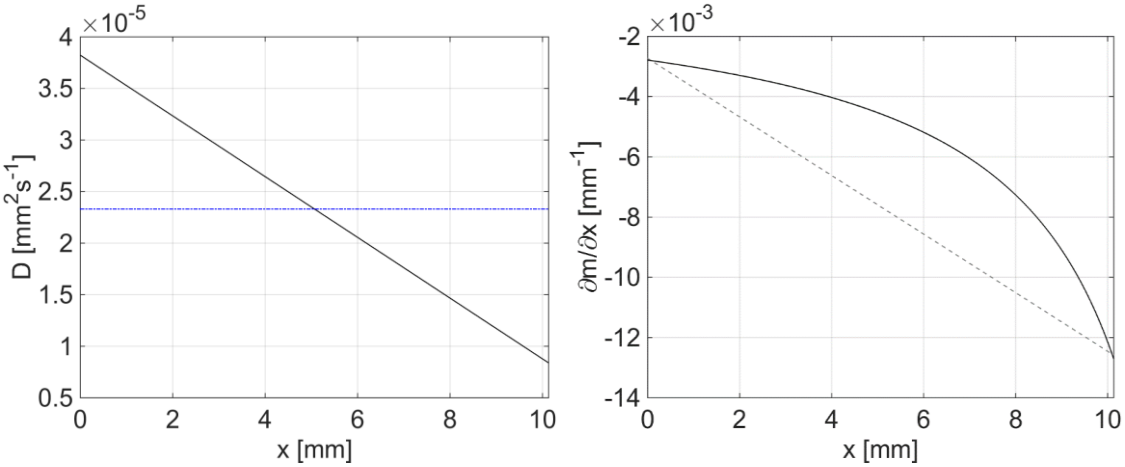

Fig. 7. Diffusion coefficient $D(m_{end},x)$, moisture gradient $\partial m/\partial x(m_{end},x)$ for the constant flux $q_m(m_{end},x)$ = 7.6E-14 kg mm^{-2}s^{-1}

Figures 5 to 7 present the results of WT dry specimen. The development of $m(x,t)$ from initial to the final state (after about 1052 h) is shown in Fig. 5. The final non-linear equilibrium distribution of $m(x,t_{end})$ is plotted in Fig. 6 against its secant to visualize the non-linearity. The average of $m(x)$ in the graph represents the quantity, which is compared to the experimentally determined global moisture content of the specimen (MC) in steady-state conditions (*cf.* Fig. 8).

Figure 7 shows the variables of Fick's first diffusion law in Eq. 10. The exponential approach of $D(m)$ leads to a linear distribution over the length section x

$$D(x)=\frac{\Delta D}{\Delta x}\cdot x+D(x=0\text{mm})\,. \tag{18}$$

Together with Eq. 12, a logarithmic distribution of the steady-state $m(x)$ is derived,

$$m(x)=\frac{1}{\alpha}\cdot\ln\left[\frac{D(x)}{D_0}\right] \qquad [-] \tag{19}$$

while the moisture flux q_m needs to be constant over the length section.

The numerically determined $D(m)$ of the final average moisture content MC_{end} leads to

$$D(MC_{end}=0.065)=2.13\cdot10^{-11} \qquad [\text{m}^2\text{s}^{-1}] \tag{20}$$

and is comparable to the experimentally determined D_{SS}.

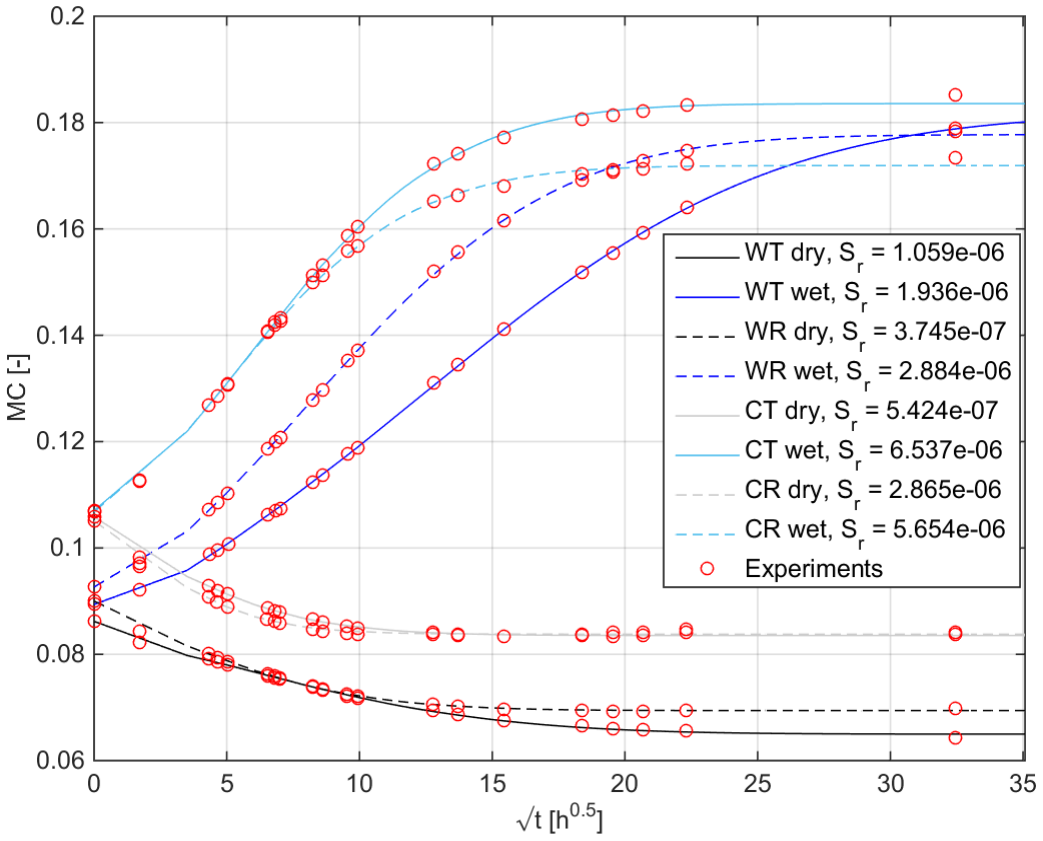

Fig. 8. Global moisture content $MC(t)$ of the investigated cup tests (*cf.* Table 1)

The results in Table 4 show an appropriate comparison in the tangential dry cup experiments with a maximum deviation of 10%. All other cup tests, however, show large deviations between the experimentally and numerically determined values. These variations may be caused by several different assumptions within the analyses. In the experimentally based calculation, $\Delta H/\Delta M$ in Eq. 6 is always assumed as a linear sorption isotherm distribution over the thickness. In fact, the sorption isotherm is a highly non-linear function and even more pronounced in high humidity, depending on the sorption direction (hysteresis) as well (Engelund *et al.* 2010). This may explain larger variations in the wet cup compared to the dry cup experiments.

During the experiment, curvature of the specimens due to moisture gradient and induced swelling was unavoidable and pronounced in wet cup tests (high moisture gradient). However, its effect on the experimental results are assumed to be negligible. The tight rubber seals (Fig. 2) ensured that the gap between the top of the cup and the wood specimens remained closed until the end of the measurement.

Moreover, a more sensitive effect such as the natural variability and the limited number of the specimens are suspected to be another reason for the incomparability between the experimental and the numerical results. As shown in Fig. 8, the *MC* varies. The initial MC_0 of walnut wood spread between $0.085 < MC_{0,walnut} < 0.095$. The final values MC_{end}, which were assumed as EMC, do not show a good agreement between R and T direction within the same wood species (Table 4). Furthermore, WT wet cup specimens still did not reach their EMC during the measurements (Fig. 8).

Additionally, the unsteady-state diffusion D_{US}, calculated by Eq. 2 for the global specimen is incomparable to any numerically obtained *D*. It is based on the continual change of mass of water versus the time interval of the unsteady experiment state (first state) and is supposed to be an easy estimation to describe the transient process until the equilibrium is reached. In the simulation, which describes more accurately the real transient and non-linear behavior, $D(MC)$ describes the continuous process in dependency of the local *m* at a certain time, *i.e.* it is applicable to determine the diffusion coefficient at every moment. Thus, $D(MC)$ is also changing simultaneously with the moisture change.

Table 6. Cup Test Specific Diffusion Coefficients $D(m)$ and the Quality of Fit with the Sum of Squared Residuals S_r (Eq. 16) and the Global Relative Error *e* (Eq. 17)

Label	Cup test	D_0	α	m_{end}	S	S_r	e
		[mm^2 s^{-1}]	[-]	[-]	[mm s^{-1}]	[-]	[%]
WT	dry	3.57E-06	27.51	0.0310	2.22E-04	1.06E-06	0.32
	wet	8.19E-06	2.091	0.2793	1.34E-05	1.94E-06	0.25
WR	dry	5.55E-06	30.61	0.0354	8.25E-04	3.75E-07	0.18
	wet	1.53E-05	3.487	0.2645	2.80E-05	2.88E-06	0.27
CT	dry	1.65E-06	41.49	0.0381	1.00E-03	5.42E-07	0.19
	wet	2.84E-05	2.373	0.2635	5.44E-05	6.54E-06	0.37
CR	dry	5.14E-06	35.80	0.0445	1.00E-03	2.87E-06	0.43
	wet	5.22E-05	0.012	0.2477	6.37E-05	5.65E-06	0.35

The applied moisture transport models fit well for the description of the global moisture contents of the specimens' *MC*. During the unsteady-state, the moisture distribution is significantly dependent on the variable $D(m)$ and could lead to imprecise

predictions of the shapes of $m(x,t)$. Since the parameters for wet cup tests (Table 6) differ from those of the respective dry cup, another approach would become necessary for the determination of universal diffusion coefficients.

The results of the inverse analyses for the fitted curves of all $MC(t)$ functions are visualized in Fig. 8 with their diffusion parameters for Eq. 12 in Table 6. The low values of the objective function S_r and the global relative errors e (Eqs. 16 and 17) verify that the determined $D(m)$ led to appropriate results in the global moisture content prediction over time. For any configuration with varying material direction, wood species, and humidity load, different parameters were determined. The differences in the first two points are physically and naturally justifiable due to anisotropy and natural variations in micro-structure and density. Furthermore, walnut has a higher extractive content, which increases the inner moisture transport resistance [*e.g.* (Wagenführ 2007)]. The different parameters for dry and wet conditions show the deficits of the applied diffusion coefficient model with respect to a universal material model of $D(m)$. While each test configuration will be represented with a minimal deviation, the general usage over the whole humidity spectrum is not appropriate. An additional investigation was carried out to determine one diffusion model for different conditions. The respective dry and wet cup specimens were considered together in one inverse analysis with a single exponential diffusion equation for both tests. Since the result showed a large error, it is not considered further. Additional investigations with respect to sorption directions and different humidity steps are necessary. Moreover, the influence of the density on $D = D(m,\rho)$ becomes visible, which needs to be considered in a further step (Eitelberger 2011).

Experimental diffusion tests on walnut and cherry wood with the cup test method have been conducted with respect to the average diffusion coefficients in unsteady- and steady-state conditions. The experiments served as a basis for an inverse analysis, coupled to an FE-simulation for the numerical determination of moisture-dependent and cup test specific diffusion coefficients $D(m)$.

The numerical diffusion model was applied to investigate the internal, time-dependent moisture profile and to assess the quality of the experimentally determined steady-state diffusion coefficients. Both the experimental D_{SS} and the numerical $D(MC)$ showed better correlation for the dry cup experiments, especially for T-direction. Large deviations between the wet cup results could have occurred due to the natural inhomogeneity and the limited number of specimens.

The determined diffusion parameters enable the simulation of the cup-test experiments. They are not universally appropriate for the prediction of transient conditions in the scope of FE-analyses with several humidity changes over the whole humidity spectrum. For a general moisture dependent diffusion model and for the consideration of the density-dependency, additional cup tests with further and smaller moisture differences considering a larger spectrum of relative humidity steps need to be tested (Gereke 2009) and further regression functions need to be assessed. Alternatively, multi-scale based approaches, like in (Eitelberger 2011) (*c.f.* configurations WT6, WT7 for walnut in Table 5) or multi-Fick'ian transport models (Konopka and Kaliske 2016) could be applied.

Further experiments in cup tests are required for a better determination of a universal single phased Fick'ian diffusion model, as presented by Olek *et al.* (2011). Alternatively, detailed analyses of local distribution of moisture content may also lead to reliable results (Hering 2011). In Mannes *et al.* (2009) and Mannes *et al.* (2012), the local moisture content of the specimens along the diffusion direction were investigated by neutron imaging. In Koc and Houska (2002) and Koc *et al.* (2003), the samples were cut

and weighted separately, leading to a discrete and rough moisture profile along the longitudinal section.

However, the results enable the comparison to similar tests with different materials, *e.g.* other wood species, wood products, or composite materials. The determined characteristics will support further investigations of composite materials, like glued wood, to analyze and to compare the different characteristics and the influence of *e.g.* bond lines in relation to specific glues, on the internal moisture transport.

CONCLUSIONS

1. The average diffusion coefficients in unsteady- and steady-state conditions for walnut and cherry wood in radial and tangential material directions were determined experimentally with the cup test method.
2. The experiments served as a basis for an inverse analysis, coupled with a FE-simulation for the numerical determination of moisture-dependent and cup test specific diffusion coefficients $D(m)$ of these wood species.
3. The numerical diffusion model was applied to investigate the internal, time-dependent moisture profile and to assess the quality of the experimentally determined steady-state diffusion coefficients. Both the experimental D_{SS} and the numerical $D(MC)$ showed better correlation for the dry cup experiments, especially for T-direction. Large deviations were observed between the wet cup results.
4. The determined diffusion parameters $D(m)$ for walnut and cherry enable the simulation of the cup-test experiments and the comparison to similar tests with different materials, *e.g.* other wood species, wood products, or composite materials, like glued wood.
5. The diffusion parameters $D(m)$ are not universally applicable for the prediction of arbitrary transient conditions in the scope of FE-analyses.

ACKNOWLEDGMENTS

The authors gratefully acknowledge the financial support by the German Research Foundation (DFG) (project KA 1163/25) and Swiss National Science Foundation (SNF) (project 14762) within the collaboration "Modelling and Characterization of the Structural Behaviour of Wooden Cultural Heritage under Hygro-mechanical Loading."

REFERENCES CITED

Avramidis, S. (1989). "Evaluation of 'three-variable' models for the prediction of equilibrium moisture content in wood," *Wood Science and Technology* 23, 251-258. DOI: 10.1007/BF00367738

Bathe, K. J. (2002). *Finite-Elemente-Methoden [Finite Element Method]*, Springer-Verlag, Berlin.

Crank, J. (1975). *The Mathematics of Diffusion*, Oxford University Press, Oxford, UK.

DIN EN ISO 12572 (2001). "Bestimmung der Wasserdampfdurchlässigkeit,"

International Standard for Organization, Geneva, Switzerland.

Eitelberger, J. (2011). *A Multi-scale Material Description for Wood Below the Fiber Saturation Point with Particular Emphasis on Wood-water Interactions*, Ph.D. Dissertation, Technische Universität Wien, Vienna, Austria.

Engelund, E., Klamer, M., and Venås, T. (2010). *Acquisition of Sorption Isotherms for Modified Woods by the Use of Dynamic Vapour Sorption Instrumentation. Principles and Practice* (IRG/WP 10-40518), The International Research Group on Wood Protection, Biarritz, France.

Gereke, T. (2009). *Moisture-induced Stresses in Cross-laminated Wood Panels*, Ph.D. Dissertation, ETH Zürich, Zurich, Switzerland.

Hanhijärvi, A. (1997). *Modelling of Creep Deformation Mechanisms in Wood*, Ph.D. Dissertation, Helsinki University of Technology, Helsinki, Finland.

Hering, S. (2011). *Charakterisierung und Modellierung der Materialeigenschaften von Rotbuchenholz zur Simulation von Holzverklebungen*, Ph.D. Dissertation, ETH Zürich, Zurich, Switzerland.

Hrcka, R. and Babiak, M. (1999). "Charakteristiky difúzie vody v drevev agáta bieleho zist'ované optimálnymi metodami," in: *Zborník prednášok. Vedecký seminár ''Drevo, štruktúra a vlastnosti''*, Zvolen, Slovakia, pp. 47-52.

Klopfer, H. (1974). *Wassertransport durch Diffusion in Feststoffen*, Bauverlag, Wiesbaden, Germany.

Koc, P. and Houska, M. (2002). "Characterization of the sorptive properties of spruce wood by the inverse identification method," *Wood Science and Technology* 36, 265-270. DOI: 10.1007/s00107-002-0311-3

Koc, P., Houska, M., and Stok, B. (2003). "Computer aided identification of the moisture transport parameters in spruce wood," *Holzforschung* 57, 533-538. DOI: 10.1515/HF.2003.079

Konopka, D. and Kaliske, M. (2016). "Hygro-mechanical FE-analysis of wooden structures: Implementation and application of reliable moisture transport models," in: *World Conference on Timber Engineering (WCTE 2016)*, Vienna, Austria.

Lamb, F. M. (1992). "Splits and cracks in wood," in: *Western Dry Kiln Association. 43rd Meeting*, Reno, NV, USA.

Mannes, D., Schmidt, J., Volkmer, T., and Niemz, P. (2012). "Untersuchungen zum Einfluss der Klebstoffart auf den kapillaren Wassertransport in Holz parallel zur Faserrichtung," *Bauphysik* 34, 61-65. DOI: 10.1002/bapi.201200007

Mannes, D., Sonderegger, W., Hering, S., Lehmann, E., and Niemz, P. (2009). "Non-destructive determination and quantification of diffusion processes in wood by means of neutron imaging," *Holzforschung* 63, 589-596. DOI: 10.1515/HF.2009.100

Olek, W., Perré, P., and Weres, J. (2005). "Inverse analysis of the transient bound water diffusion in wood," *Holzforschung* 59, 38-45. DOI: 10.1515/HF.2005.007

Olek, W., Perré, P., and Weres, J. (2011). "Implementation of a relaxation equilibrium term in the convective boundary condition for a better representation of the transient bound water diffusion in wood," *Wood Science and Technology* 45, 677-691. DOI: 10.1007/s00226-010-0399-2

Pfriem, A. (2006). *Untersuchungen zum Materialverhalten thermisch modifizierter Hölzer für deren Verwendung im Musikinstrumentenbau*, Dissertationsschrift, Technische Universität Dresden, Dresden, Germany.

Reichel, S. (2015). *Modellierung und Simulation hygro-mechanisch beanspruchter Strukturen aus Holz im Kurz- und Langzeitbereich*, Dissertationsschrift, Technische

Universität Dresden, Dresden, Germany.
Siau, J. (1995). *Wood: Influence of Moisture on Physical Properties*, Department of Wood Science and Forest Products, Virginia Polytechnic Institute and State University, Blacksburg, VA, USA.
Sonderegger, W. (2011). *Experimental and Theoretical Investigations on the Heat and Water Transport in Wood and Wood-based Materials*, Ph.D. Dissertation, ETH Zürich, Zurich, Switzerland.
Sonderegger, W. and Niemz, P. (2009). "Thermal conductivity and water vapour transmission properties of wood-based materials," *European Journal of Wood and Wood Products* 67, 313-321. DOI: 10.1007/s00107-008-0304-y
Sonderegger, W., Vecellio, M., Zwicker, P., and Niemz, P. (2011). "Combined bound water and water vapour diffusion of Norway spruce and European beech in and between the principal anatomical directions," *Holzforschung* 65, 819-828. DOI: 10.1515/HF.2011.091
Wadsö, L. (1994). "Unsteady-state water vapor adsorption in wood: An experimental study," *Wood and Fiber Science* 26:36-50.
Wagenführ, R. (2007). *Holzatlas*, Fachbuchverlag Leipzig, Leipzig, Germany.

Article submitted: June 26, 2017; Peer review completed: September 4, 2017; Revised version received and accepted: September 26, 2017; Published: October 10, 2017.
DOI: 10.15376/biores.12.4.8920-8936